Hindawi
Journal of Chemistry
Volume 2019, Article ID 2858170, 7 pages
https://doi.org/10.1155/2019/2858170

Research Article

Fast and Effective Route for Removing Methylene Blue from Aqueous Solution by Using Red Mud-Activated Graphite Composites

Ha Xuan Linh,[1] Ngo Thi Thu,[2] Tran Quoc Toan,[2] Do Tra Huong,[2] Bui Thanh Giang,[2] Huynh Ky Phuong Ha,[3] Hong-Tham T. Nguyen,[4] N. T. K. Chung,[5] Tri Khoa Nguyen,[4] and Nguyen Thanh Hai[6,7]

[1]*International School-Thai Nguyen University, Thai Nguyen, Vietnam*
[2]*Department of Chemistry, Thai Nguyen University of Education, Thai Nguyen, Vietnam*
[3]*Faculty of Chemical Engineering, Ho Chi Minh City University of Technology, Ho Chi Minh City, Vietnam*
[4]*NTT Hi-Tech Institute, Nguyen Tat Thanh University, 300A Nguyen Tat Thanh, District 4, Ho Chi Minh City 755414, Vietnam*
[5]*Department of Physics, Thu Dau Mot University, 6 Tran Van on Street, Thu Dau Mot, 820000 Binh Duong Province, Vietnam*
[6]*Research and Development Center for Advanced Technology, Hanoi, Vietnam*
[7]*Nanotechnology Program, VNU Vietnam-Japan University, Hanoi, Vietnam*

Correspondence should be addressed to Tri Khoa Nguyen; nguyentrikhoa702@gmail.com and Nguyen Thanh Hai; haidhsp95@gmail.com

Received 14 March 2019; Accepted 29 May 2019; Published 1 July 2019

Guest Editor: Van Duong Dao

In this work, the mixture of red mud slurry and inorganic salt ($(NH_4)_2SO_4$) has been used as an electrolyte for electrochemical activation of graphite. The red mud-activated graphite composite was then used as an adsorbent for removing methylene blue from aqueous solution by the batch method. The effect of pH, contact time, adsorbent dosage, and the initial concentration of methylene blue was investigated. The optimal condition was found at pH 6, contact time 120 min, and amount of adsorbent 1 mg/L. The maximum adsorption capacity was found to be 89.28 mg/g based on the Langmuir isotherm equation, suggesting that the red mud-activated graphite composite is a very potential adsorbent for removing methylene blue and is also used in other coloured wastewater treatments.

1. Introduction

Dyes and pigments (e.g., methylene blue (MB)) are widely used in textile, dyeing, printing, and coating industries. Their wastewater contains a high concentration of non-biodegradable organic compounds which can cause long-term health effects on human beings and animals and significantly qualitative changes in the environment [1]. Therefore, it is essential to remove the contaminants such as dyes and heavy metal ions in the wastewater before discharging into the water source. Several methods such as biodegradation, chemical treatment, the use of UV and ozone, and adsorption have been applied to get rid of MB from wastewater [2–6]. Among them, the utilization of agricultural or industrial by-products as adsorbents for wastewater treatment has received lots of attention [7]. Recently, chemically or thermally activated seawater neutralized treated red mud (RM) has been effectively used as a promising candidate for removing heavy metal ions and dyes from aqueous solution as a result of the reaction between the hydroxyl groups and active site on red mud or through adsorption onto external surfaces [8, 9]. Besides, the application of graphene oxide (GO) or graphene nanosheets (GSs) adsorbent has been shown to be a simple and effective method for the removal of dye contaminants from wastewater [1, 10]. Moreover, the modification of graphene under

basic conditions or the combination of graphene with other metal oxides showed a great potential for removal of heavy metals ions in water [11–13]. In order to generate porosity for adsorptive purposes, the activation of graphite using alkaline hydroxides such as KOH or NaOH usually requires concentrated alkali solution, long reaction time, and high temperature [14, 15]. Therefore, finding a simple, effective, and energy-saving process for producing activated graphite materials is highly demanded.

As previously discussed, red mud with a high basic property must be activated simultaneously with other materials [16], using acidic conditions [17] or high temperature [18] before utilization. Also, $(NH_4)_2SO_4$ solution has been demonstrated to be an effective electrolyte for one-step fast electrochemical exfoliation of graphite [19]. These works show a great possibility of using the mixture of RM slurry and $(NH_4)_2SO_4$ as an electrolyte for activating graphite. Therefore, in this study, we combine red mud slurry with $(NH_4)_2SO_4$ as an electrolyte for simultaneous activation and exfoliation of graphite and employ the as-product for removing MB from aqueous solution.

2. Materials and Methods

2.1. Synthesis and Characterization of Materials. 300 mL of red mud slurry (Tan Rai factory, Lam Dong Province, Vietnam) was added with 100 mL of 5% w/w $(NH_4)_2SO_4$ solution under a magnetic stirrer to form a homogeneous electrolyte at pH 14. Graphite rod was then activated by electrochemical exfoliation using this electrolyte with the voltage of 15 V and temperature from 50–70°C for 120 min (Scheme 1). The beaker was cooled to room temperature in 1 h, and the material was filtrated and washed with DI water until natural pH is reached. The obtained material was finally put in drying oven at 150°C for 24 h and placed in a desiccator at 25°C (denoted as RMGC). The activated graphite without red mud (named as electrochemically exfoliated graphite (EEG)) was also prepared for the comparison purpose using conventional electrolytic solution at pH 14 (200 mL of 7.5% KOH and 50 mL of 5% $(NH_4)_2SO_4$, pH 14).

XRD patterns were characterized by using a diffractometer (D2 PHASER using Cu Kα radiation). RMGC and EEG structures were examined using high-resolution confocal Raman microscopy (HORIBA, Lab RAM HR 800 equipped with a 514.5 nm Ar laser source). Morphology of materials was determined by using a high-resolution transmission electron microscope (HRTEM, JEOL 2100F apparatus operated at 200 kV). Field emission scanning electron microscopy (SEM) images were collected using the JEOL JSM-6500F scanning electron microscope operated at 15 kV.

2.2. Adsorption Studies. The adsorption experiments for RMGC were carried out by the batch method at room temperature. Several factors including contact time (0 to 270 minutes), initial MB concentration (10, 25, 50, 75, and 100 mg/L), amount of adsorbent (0.01–0.1 g), and solution pH (2.0–12.0) were investigated. The solution of 10% HCl and 0.1 M NaOH was used to adjust pH solution before addition of the adsorbent. After the test periods, the samples were separated by centrifugation for 15 min at 4000 rpm and the collected supernatant determined the concentration of MB by absorbance measurement using a UV-Vis spectrophotometer (Hitachi UH5300) at a wavelength of 665 nm.

pH_{pzc} (the point of zero charge) of the RMGC was determined in a similar method as Faria et al. [10] At first, 25 mL of 0.01 M NaCl solution was prepared and added into conical flasks, and the pH solution was adjusted by adding NaOH and HCl solutions from 2 to 12. After that, each conical flask was added 0.1 g of the obtained material and shaken for 48 h at room temperature. After the tests, the pH solution was redetermined and denoted as the final pH. Concomitantly, the difference between the initial pH and final pH (initial pH—final pH) was plotted against the initial pH. The point at which the resulting curve intersected with abscissa was pH_{pzc} of the RMGC.

The adsorption capacity and removal efficiency of MB on RMGC was calculated by the following equation:

$$q = \frac{(C_0 - C_e)V}{M},$$
$$R\,\% = \frac{(C_0 - C_e)}{C_0} \times 100\%, \quad (1)$$

where V (L) is the solvent volume and M (g) is the mass of adsorbent. C_0 and C_e (mg/L) are initial and equilibrium concentrations, respectively. q (mg/g) is the adsorption capacity at equilibrium time, and R (%) is the removal efficiency of MB.

Adsorption isotherms were conducted at pH 6, contact time 120 min, and room temperature. The different initial concentrations of MB (10, 25, 50, 75, and 100 mg/L) were experimented to analyse the data. The isotherm models of Freundlich and Langmuir are expressed by the following equations:

$$\text{Freundlich: } q_e = K_f C_e^{1/n},$$
$$\text{Langmuir: } q_e = \frac{q_0 b C_e}{1 + bC_e}, \quad (2)$$

where K_f and n are Freundlich constants related to sorption capacity and sorption intensity of adsorbent. q_e and C_e are the adsorption capacity and concentration at equilibrium of MB in solution, respectively. q_0 and b are the monolayer adsorption capacity and the Langmuir constant.

3. Results and Discussion

3.1. Structural Analysis. To investigate the morphology of the materials, SEM micrographs are depicted in Figure 1. EEG image displayed flattened morphology and turned into a particle-on-sheet structure in RMGC after exfoliating, which can be further observed by the TEM image in Figure 2. Clearly, exfoliated graphite flakes were overlapped with nanoparticles, which were fairly uniformly distributed on its surface layer (Figure 1(c)). In situ EDS also revealed that the

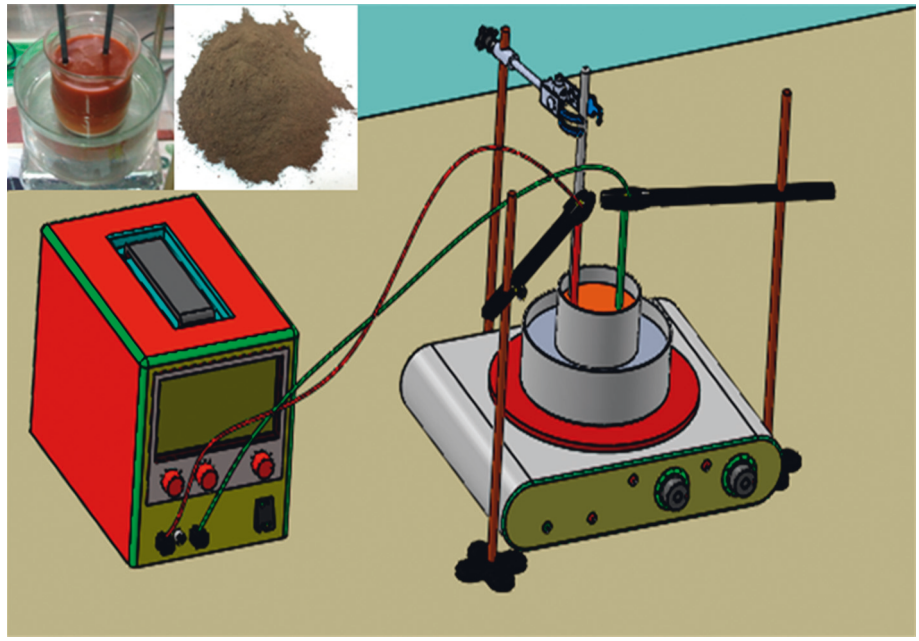

Scheme 1: Schematic of RMGC formation (the inset is the working system and as-product).

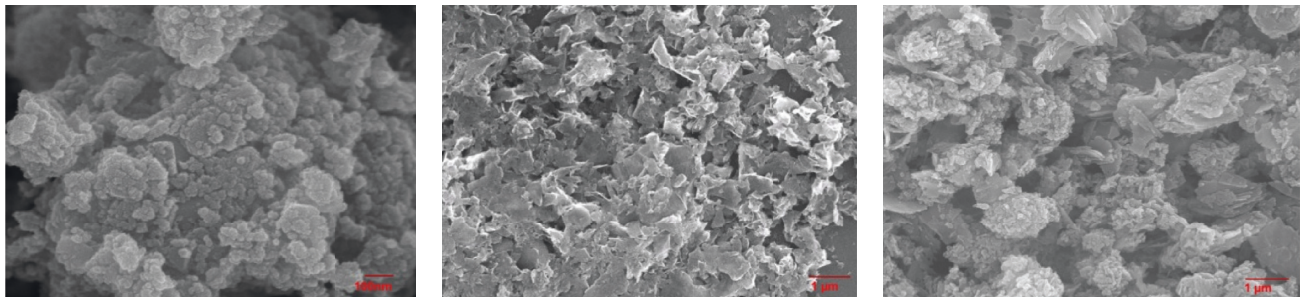

(a) (b) (c)

Figure 1: SEM images of (a) RM, (b) EEG, and (c) RMGC.

RMGC mainly consisted of C, O, Fe, Si, and Al elements (Figure 2).

The XRD patterns of all collected materials are displayed in Figure 3. The EEG pattern shows a sharp and high-intensity peak at a value of 2θ of 26.6°, indexing to the 002 reflection. In addition, there are three small peaks at values of 2θ of 42.8, 21.6, and 34.6°, indexing to the 100, 101, and 004 reflections, respectively. After exfoliating, these peaks still remained, while new small peaks appeared at 2θ values of 18.1, 21.3, 29.6, 33.1, 35.6, 37.1, 54.2, 62.2, and 64.3°. These new peaks can be assigned to the phases of quartz ($Qz = SiO_2$), gibbsite ($Gb = \gamma\text{-}Al(OH)_3$), goethite ($Gt = \alpha\text{-}FeOOH$), and hematite ($Hm = Fe_2O_3$) [13]. Raman spectroscopy was used to further verify the structure of RMGC. As shown in Figure 4, the characteristic peaks of exfoliated graphite flakes were D- and G-band at 1573 cm^{-1} and 1583 cm^{-1}, respectively, also presented in RMGC [20]. Previously, the OH^- ions will initially oxidize graphite at the edge and/or grain boundaries and were proposed to expand the distance between graphite layers as well as for the following anion intercalation. Concretely, the sulfate ions SO_4^{2-} intercalate and facilitate in separating weakly bonded graphite layers [19]. In addition, RM is a heterogeneous mixture of fine-grained solids, mainly consisting of hematite, gibbsite, quartz, titanium oxide, carbonates, and desalination products (e.g., cancrinite and sodalite) with high alkalinity, resulted in the exits of hydrated OH^- together with SO_4^{2-} ions. We considered that applying bias voltage, oxygen evolution of SO_4^{2-} and OH^- ions could attach the edge sites and grain boundaries of graphitic layers, which eventually lead to exfoliation including activation with fine RM particles.

3.2. Adsorption Studies. The effect of pH on the RMGC's adsorption of MB is shown in Figure 5. In pH range of 2 to 6, it is obvious that the removal efficiency increased rapidly and was then stable when pH increased from 6 to 12. In the pH drift test (Figure 5(b)), the pH_{pzc} value of the RMGC was observed at 8.3 ± 0.1. At lower pH, a large number of H^+ ions compete with cationic dye for adsorption sites on RMGC. Moreover, the presence of H^+ ions could protonate the

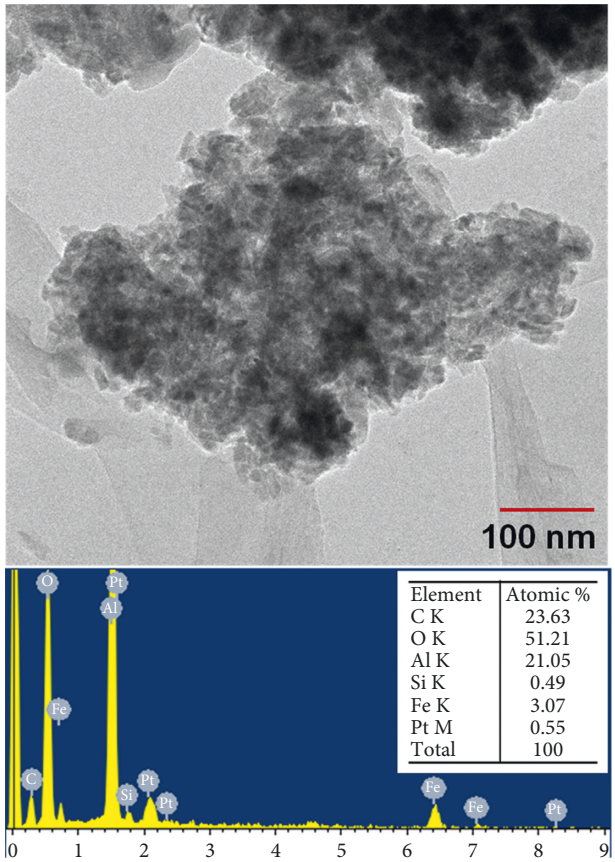

Figure 2: TEM image of RMGC, EDS spectrum of RMGC.

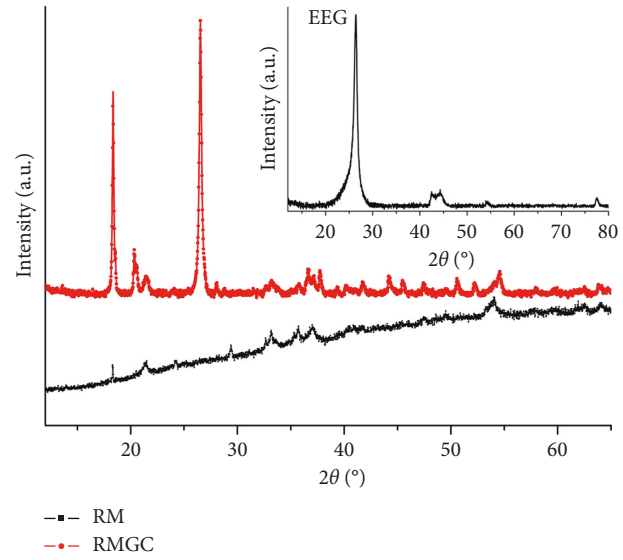

Figure 3: XRD patterns of RM and RMGC (inset is that of EEG).

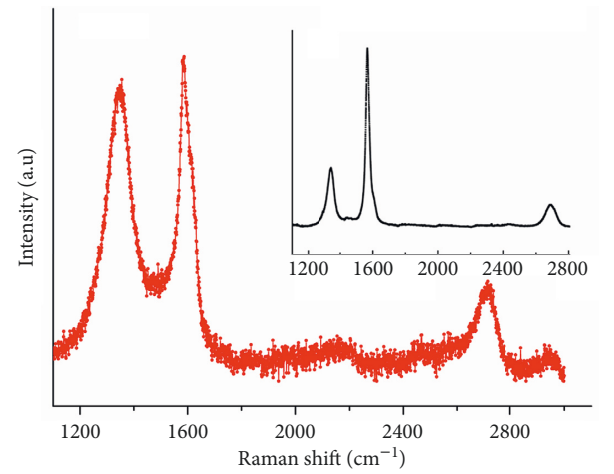

Figure 4: Raman spectrum of RMGC (inset is that of EEG).

functional groups of the graphene and further decreases the adsorption amount of MB. On the contrary, the deprotonation of surface groups at a higher pH would increase the negative charges on the surface, which could result in a greater adsorption amount of MB. Therefore, the electrostatic attraction is responsible for adsorption of MB on RMGC, and the mechanism is proposed as follows:

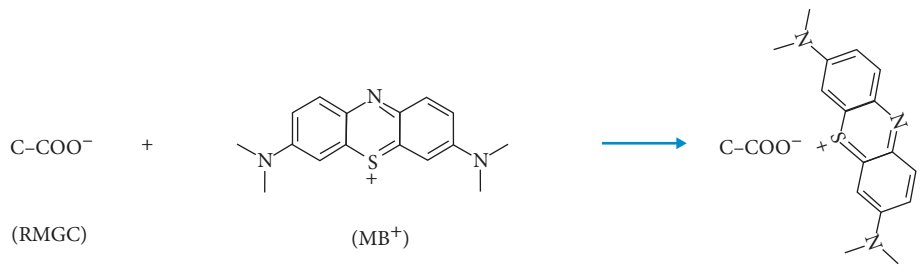

The highest removal efficiency of MB on RMGC was at pH = 6. In the actual environment, the wastewater generally occurs at the neutral pH value. Thus, the pH value for further experiments was from 5 to 6.

To determine the equilibrium time of removal of MB on RMGC, time intervals up to 270 min of experiment were conducted. As can be seen from Figure 6, MB was rapidly absorbed after 120 min at a removal efficiency of 96.02% but slowed down gradually when reached equilibrium. The reason could be explained by the availability of active sites during the adsorption process, generally in the first stage and after a certain time period of adsorption. Specifically, the active sites

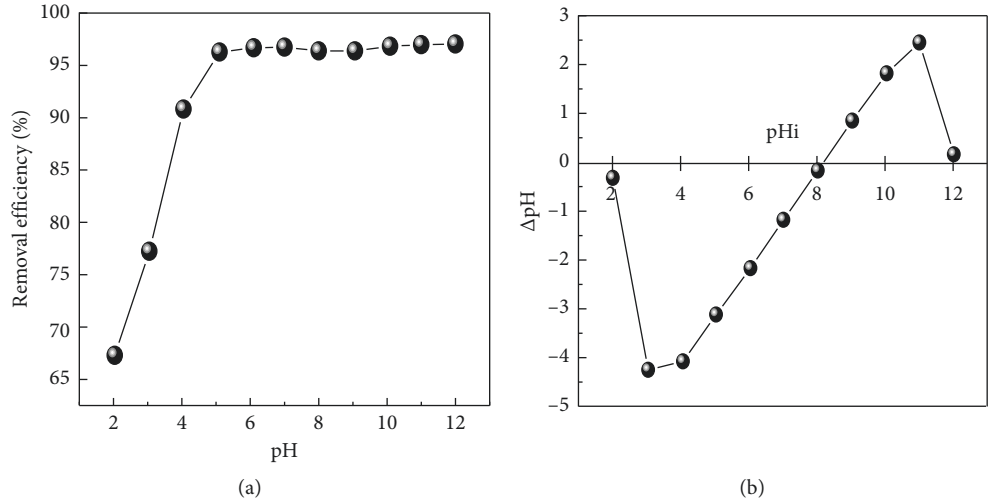

Figure 5: (a) Effect of pH value on MB adsorption and (b) pH_{pzc} (MB concentration: 50 mg/L; adsorbent dose: 0.05 g).

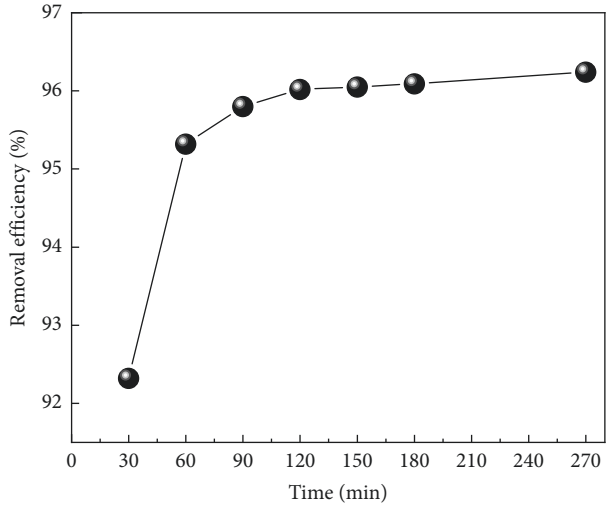

Figure 6: Effect of contact time on MB adsorption (MB concentration: 50 mg/L; adsorbent dose: 0.05 g).

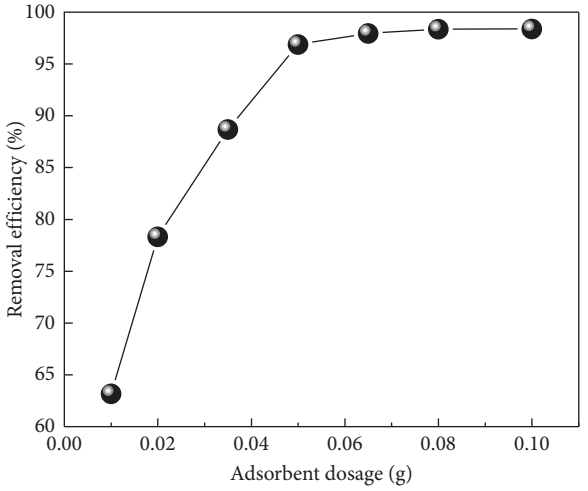

Figure 7: Effect of adsorbent dosage on MB adsorption (MB concentration: 50 mg/L; time: 120 min).

will be settled by MB molecules when contact time is increased. At a certain time, the active sites will be fully occupied and could cause to create a repulsive force between the adsorbate on the adsorbent surface and in the bulk phase. After equilibrium conditions are attained, the removal efficiency kept was almost invariable. The contact time at 120 min was preferred as the equilibrium time for further experiments.

Figure 7 illustrates the effect of adsorbent dosage on MB removal efficiency using RMGC. It can be clear that the removal efficiency of MB gradually rised with an increase in an adsorbent dosage up to 0.05 g and thereafter remained unchanged. The more the adsorbent dosage could be added, the more the active sites are available. As a result, the more vacant surface sites were utilized at a fixed MB concentration. The amount of adsorbent was chosen to be 0.05 g for further experiments.

Figure 8 presents the effect of initial concentration on the adsorption of MB on RMGC, revealing that removal efficiency decreased from 98.75 to 84.16% as the MB concentration increased from 50 to 250 mg/L, as a result of the progressive increase in the electrostatic interaction between MB and RMGC active sites. Under these circumstances, the active sites were covered since MB concentration increases. Additionally, the higher initial concentrations lead to an increase in the affinity of the cationic dyes towards the active sites.

The relative isotherm parameters and correlation coefficient (R^2) values are listed in Table 1. The analyzed data suggested that MB adsorption could be described in the Langmuir model than the Freundlich model since its R^2 value was higher. This demonstrated that the adsorption of MB on RMGC was monolayer adsorption and controlled by a homogeneous process. Additionally, the maximum capacity (q_{max}) of MB adsorbed on RMGC was predicted as 89.28 mg/g, which was similar to some other adsorbents [21, 22]. The

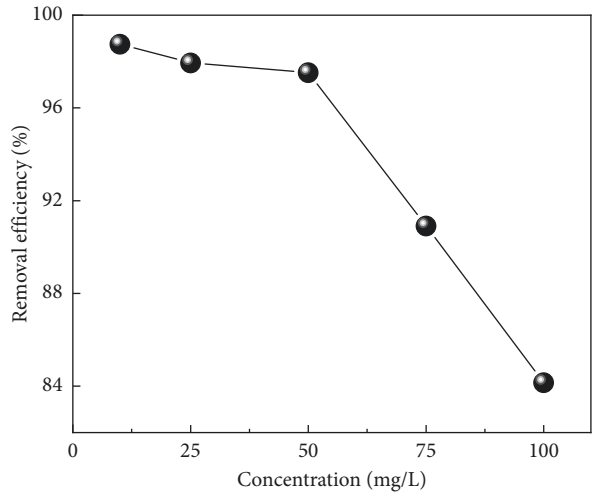

Figure 8: Effect of initial concentration on MB adsorption (adsorbent dose: 0.05 g; time: 120 min).

Table 1: Adsorption isotherm constants for the adsorption of MB by RMGC.

Model	Parameters	Value
Langmuir	q_{max} (mg/g)	89.28
	b (L/mg)	0.77
	R^2	0.9995
Freundlich	n	2.315
	K_f (mg/g)/(mg/L)^n	30.489
	R^2	0.894

Table 2: Comparison of RMGC with other adsorbents.

Adsorbents	pH	Time	q_{max} (mg/g)	References
Charcoal	—	~6 h	67.2	[21]
Fibrous clay minerals	4	24 h	85.5	[22]
Graphene/Fe_3O_4 composites	2–11	20 min	43.82	[23]
Graphene/carbon nanotube	6-7	180 min	81.97	[24]
RMGC	6	120 min	89.28	This work

—, no information.

comparison of q_{max} and experimental conditions of various adsorbents is given in Table 2.

4. Conclusions

The adsorbent of red mud-activated graphite composites (RMGC) was successfully prepared via electrochemical exfoliation of graphite in the mixture of RM slurry and $(NH_4)_2SO_4$ as an electrolyte and applied for the adsorption of methylene blue in aqueous solution. The optimal conditions for removal of MB were at pH 6 and 120 min. According to the Langmuir model, the maximum adsorption capacity was found to be 89.28 mg/g. The RMGC has proven to be an effective low-cost adsorbent for the removal of MB, which could be studied extensively in order to apply it for wastewater treatment in the future.

Data Availability

No data were used to support this study.

Conflicts of Interest

The authors declare that there are no conflicts of interest regarding the publication of this paper.

References

[1] M. Yusuf, F. M. Elfghi, S. A. Zaidi, E. C. Abdullah, and M. A. Khan, "Applications of graphene and its derivatives as an adsorbent for heavy metal and dye removal: a systematic and comprehensive overview," *RSC Advances*, vol. 5, no. 62, pp. 50392–50420, 2015.

[2] M. Dezfoolian, F. Rashchi, and R. K. Nekouei, "Synthesis of copper and zinc oxides nanostructures by brass anodization in alkaline media," *Surface and Coatings Technology*, vol. 275, pp. 245–251, 2015.

[3] B. Hameed, A. Din, and A. Ahmad, "Adsorption of methylene blue onto bamboo-based activated carbon: kinetics and equilibrium studies," *Journal of Hazardous Materials*, vol. 141, no. 3, pp. 819–825, 2007.

[4] P. T. P. Hoa, S. Managaki, N. Nakada et al., "Antibiotic contamination and occurrence of antibiotic-resistant bacteria in aquatic environments of northern Vietnam," *Science of the Total Environment*, vol. 409, no. 15, pp. 2894–2901, 2011.

[5] D. K. Padhi, K. M. Parida, and S. K. Singh, "Mechanistic aspects of enhanced Congo red adsorption over graphene oxide in presence of methylene blue," *Journal of Environmental Chemical Engineering*, vol. 4, no. 3, pp. 3498–3511, 2016.

[6] O. Legrini, E. Oliveros, and A. M. Braun, "Photochemical processes for water treatment," *Chemical Reviews*, vol. 93, no. 2, pp. 671–698, 1993.

[7] N. Nasuha and B. H. Hameed, "Adsorption of methylene blue from aqueous solution onto NaOH-modified rejected tea," *Chemical Engineering Journal*, vol. 166, no. 2, pp. 783–786, 2011.

[8] M. Starowicz and B. Stypuła, "Electrochemical synthesis of ZnO nanoparticles," *European Journal of Inorganic Chemistry*, vol. 2008, no. 6, pp. 869–872, 2008.

[9] S. Wang, Y. Boyjoo, A. Choueib, and Z. H. Zhu, "Removal of dyes from aqueous solution using fly ash and red mud," *Water Research*, vol. 39, no. 1, pp. 129–138, 2005.

[10] P. C. C. Faria, J. J. M. Órfão, and M. F. R. Pereira, "Adsorption of anionic and cationic dyes on activated carbons with different surface chemistries," *Water Research*, vol. 38, no. 8, pp. 2043–2052, 2004.

[11] Y. Li, M. van Zijll, S. Chiang, and N. Pan, "KOH modified graphene nanosheets for supercapacitor electrodes," *Journal of Power Sources*, vol. 196, no. 14, pp. 6003–6006, 2011.

[12] J. G. S. Moo, B. Khezri, R. D. Webster, and M. Pumera, "Graphene oxides prepared by hummers', hofmann's, and staudenmaier's methods: dramatic influences on heavy-metal-ion adsorption," *ChemPhysChem*, vol. 15, no. 14, pp. 2922–2929, 2014.

[13] D. N. H. Tran, S. Kabiri, L. Wang, and D. Losic, "Engineered graphene–nanoparticle aerogel composites for efficient removal of phosphate from water," *Journal of Materials Chemistry A*, vol. 3, no. 13, pp. 6844–6852, 2015.

[14] T.-T.-N. Nguyen and J. L. He, "Preparation of titanium monoxide nanopowder by low-energy wet ball-milling," *Advanced Powder Technology*, vol. 27, no. 4, pp. 1868–1873, 2016.

[15] T. Kim, G. Jung, S. Yoo, K. S. Suh, and R. S. Ruoff, "Activated graphene-based carbons as supercapacitor electrodes with macro- and mesopores," *ACS Nano*, vol. 7, no. 8, pp. 6899–6905, 2013.

[16] H. S. Altundoğan, S. Altundoğan, F. Tümen, and M. Bildik, "Arsenic adsorption from aqueous solutions by activated red mud," *Waste management*, vol. 22, no. 3, pp. 357–363, 2002.

[17] M. P. Elizalde-González, J. Mattusch, W.-D. Einicke, and R. Wennrich, "Sorption on natural solids for arsenic removal," *Chemical Engineering Journal*, vol. 81, no. 1–3, pp. 187–195, 2001.

[18] S. J. Palmer, M. Nothling, K. H. Bakon, and R. L. Frost, "Thermally activated seawater neutralised red mud used for the removal of arsenate, vanadate and molybdate from aqueous solutions," *Journal of Colloid and Interface Science*, vol. 342, no. 1, pp. 147–154, 2010.

[19] K. Parvez, Z.-S. Wu, R. Li et al., "Exfoliation of graphite into graphene in aqueous solutions of inorganic salts," *Journal of the American Chemical Society*, vol. 136, no. 16, pp. 6083–6091, 2014.

[20] A. C. Ferrari, J. C. Meyer, V. Scardaci et al., "Raman spectrum of graphene and graphene layers," *Physical Review Letters*, vol. 97, no. 18, article 187401, 2006.

[21] F. Banat, S. Al-Asheh, R. Al-Ahmad, and F. Bni-Khalid, "Bench-scale and packed bed sorption of methylene blue using treated olive pomace and charcoal," *Bioresource Technology*, vol. 98, no. 16, pp. 3017–3025, 2007.

[22] M. Hajjaji, A. Alami, and A. E. Bouadili, "Removal of methylene blue from aqueous solution by fibrous clay minerals," *Journal of Hazardous Materials*, vol. 135, no. 1–3, pp. 188–192, 2006.

[23] L. Ai, C. Zhang, and Z. Chen, "Removal of methylene blue from aqueous solution by a solvothermal-synthesized graphene/magnetite composite," *Journal of Hazardous Materials*, vol. 192, no. 3, pp. 1515–1524, 2011.

[24] L. Ai and J. Jiang, "Removal of methylene blue from aqueous solution with self-assembled cylindrical graphene–carbon nanotube hybrid," *Chemical Engineering Journal*, vol. 192, pp. 156–163, 2012.